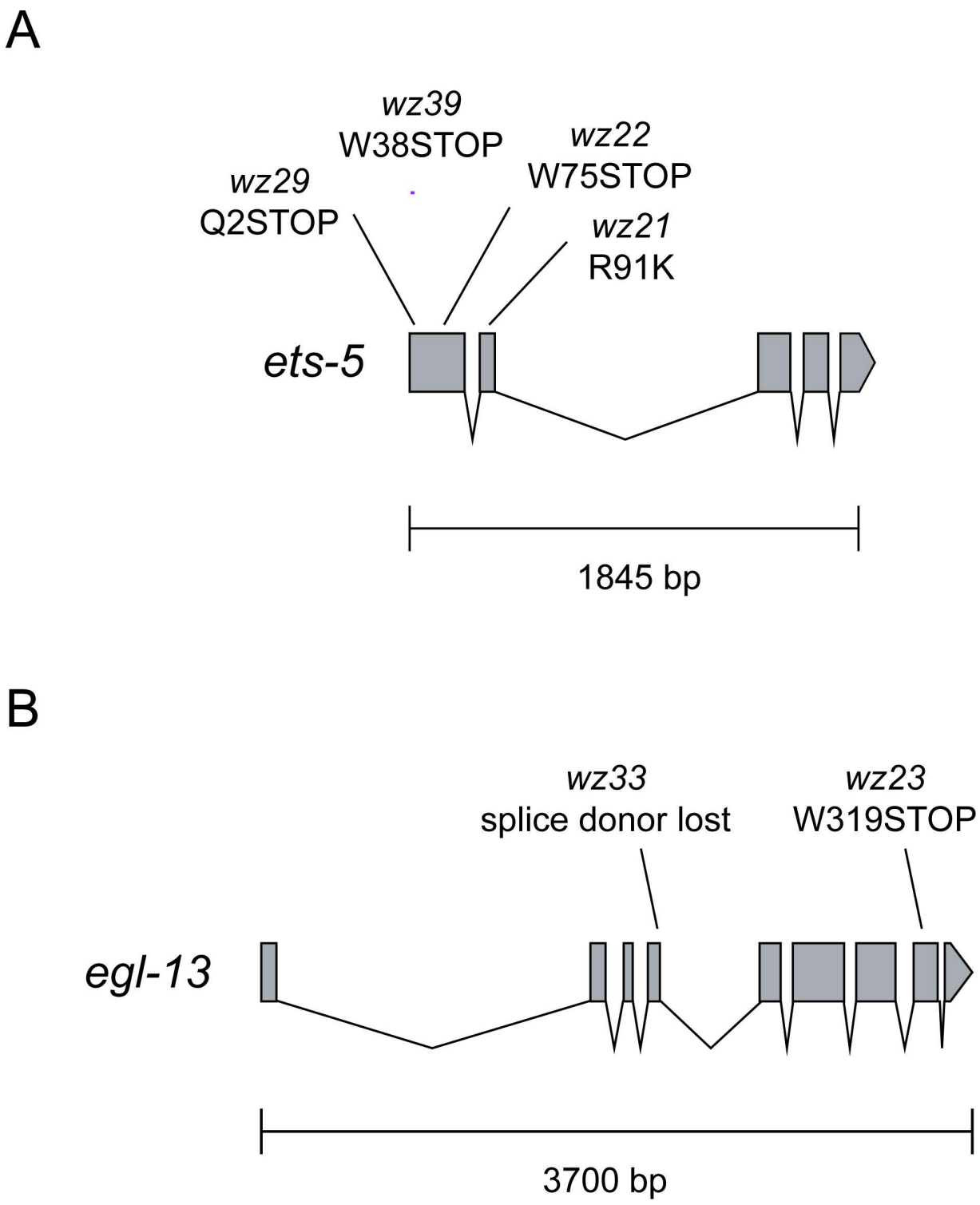

Figure S1. Alleles of *ets-5* and *egl-13* isolated by a screen for mutants with defective expression of a BAG fate marker.
A. Alleles of *ets-5* recovered from a screen for mutants with defective expression of the BAG fate marker $P_{flp\text{-}17}$*::gfp*.
B**.** Alleles of *egl-13* recovered from the same screen.

A

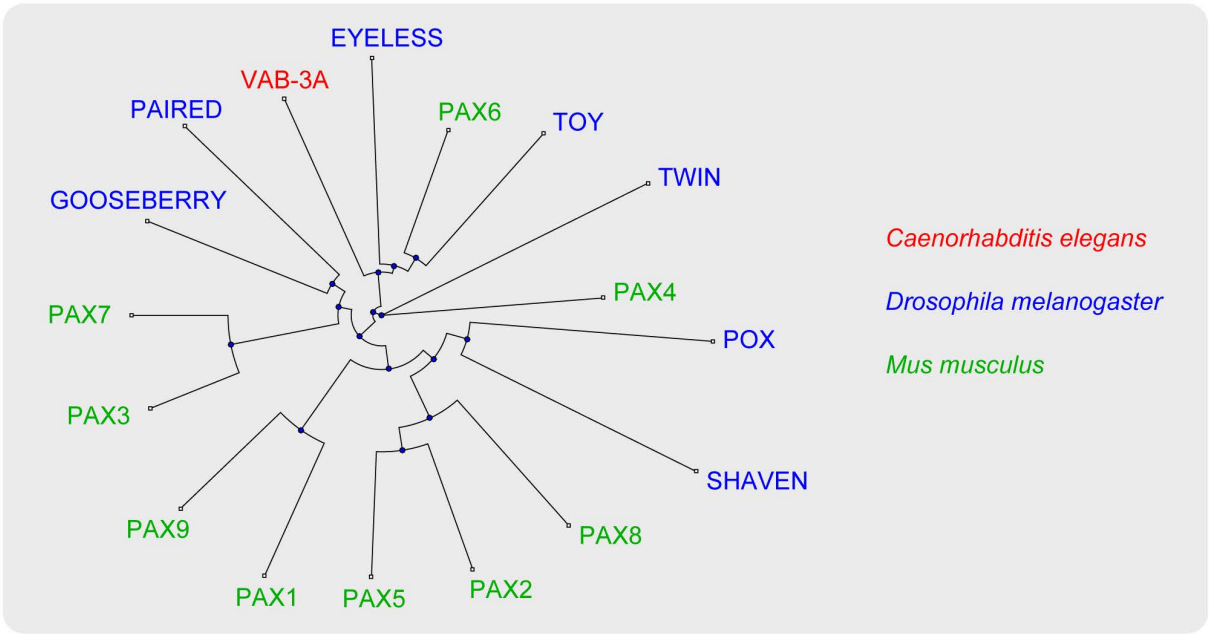

B

wz25

```
Dm POX          TGQAGVNQLGGVFVNGRPLPDCVRRRIVDLALCGVRPCDISRQLLVSHGCVSKILTRFYETGSIRPGSIGGSKTKQVATPTVVKKIIRLKEENSGMFAWEIREQLQ
Mm PAX1         QTYGEVNQLGGVFVNGRPLPNAIRLRIVELAQLGIRPCDISRQLRVSHGCVSKILARYNETGSILPGAIGGSKPR-VTTPNVVKHIRDYKQGDPGIFAWEIRDRLL
Mm PAX9         PAFGEVNQLGGVFVNGRPLPNAIRLRIVELAQLGIRPCDISRQLRVSHGCVSKILARYNETGSILPGAIGGSKPR-VTTPTVVKHIRTYKQRDPGIFAWEIRDRLL
Dm SHAVEN       DGHGGVNQLGGVFVNGRPLPDVVRQRIVELAHNGVRPCDISRQLRVSHGCVSKILSRYYETGSFKAGVIGGSKPK-VATPPVVDAIANYKRENPTMFAWEIRDRLL
Mm PAX8         SGHGGLNQLGGAFVNGRPLPEVVRQRIVDLAHQGVRPCDISRQLRVSHGCVSKILGRYYETGSIRPGVIGGSKPK-VATPKVVEKIGDYKRQNPTMFAWEIRDRLL
Mm PAX2         HRHGGVNQLGGVFVNGRPLPDVVRQRIVELAHQGVRPCDISRQLRVSHGCVSKILGRYYETGSIKPGVIGGSKPK-VATPKVVDKIAEYKRQNPTMFAWEIRAQLL
Mm PAX5         TGHGGVNQLGGVFVNGRPLPDVVRQRIVELAHQGVRPCDISRQLRVSHGCVSKILGRYYETGSIKPGVIGGSKPK-VATPKVVEKIAEYKRQNPTMFAWEIRDRLL
Mm PAX3         LGQGRVNQLGGVFINGRPLPNHIRHKIVEMAHHGIRPCVISRQLRVSHGCVSKILCRYQETGSIRPGAIGGSKPKQVTTPDVEKKIEEYKRENPGMFSWEIRDKLL
Mm PAX7         LGQGRVNQLGGVFINGRPLPNHIRHKIVEMAHHGIRPCVISRQLRVSHGCVSKILCRYQETGSIRPGAIGGSKPRQVATPDVEKKIEEYKRENPGMFSWEIRDRLL
Dm GOOSEBERRY   QGQGRVNQLGGVFINGRPLPNHIRRQIVEMAAAGVRPCVISRQLRVSHGCVSKILNRFQETGSIRPGVIGGSKPR-VATPDIESRIEELKQSQPGIFSWEIRAKLI
Dm PAIRED       SGQGRVNQLGGVFINGRPLPNNIRLKIVEMAADGIRPCVISRQLRVSHGCVSKILNRYQETGSIRPGVIGGSKPR-IATPEIENRIEEYKRSSPGMFSWEIREKLI
Mm PAX4         DGLSSVNQLGGLFVNGRPLPLDTRQQIVQLAIRGMRPCDISRSLKVSNGCVSKILGRYYRTGVLEPKCIGGSKPR-LATPAVVARIAQLKDEYPALFAWEIQHQLC
Ce VAB-3A       AGHTGVNQLGGVFVNGRPLPDATRQRIVDLAHKGCRPCDISRLLQVSNGCVSKILCRYYESGTIRPRAIGGSKPR-VATSDVVEKIEDYKRDQPSIFAWEIRDKLL
Dm EYELESS      KGHSGVNQLGGVFVGGRPLPDSTRQKIVELAHSGARPCDISRILQVSNGCVSKILGRYYETGSIRPRAIGGSKPR-VATAEVVSKISQYKRECPSIFAWEIRDRLL
Mm PAX6         NSHSGVNQLGGVFVNGRPLPDSTRQKIVELAHSGARPCDISRILQVSNGCVSKILGRYYETGSIRPRAIGGSKPR-VATPEVVSKIAQYKRECPSIFAWEIRDRLL
Dm TOY          AGHSGINQLGGVYVNGRPLPDSTRQKIVELAHSGARPCDISRILQVSNGCVSKILGRYYETGSIKPRAIGGSKPR-VATTPVVQKIADYKRECPSIFAWEIRDRLL
```

C

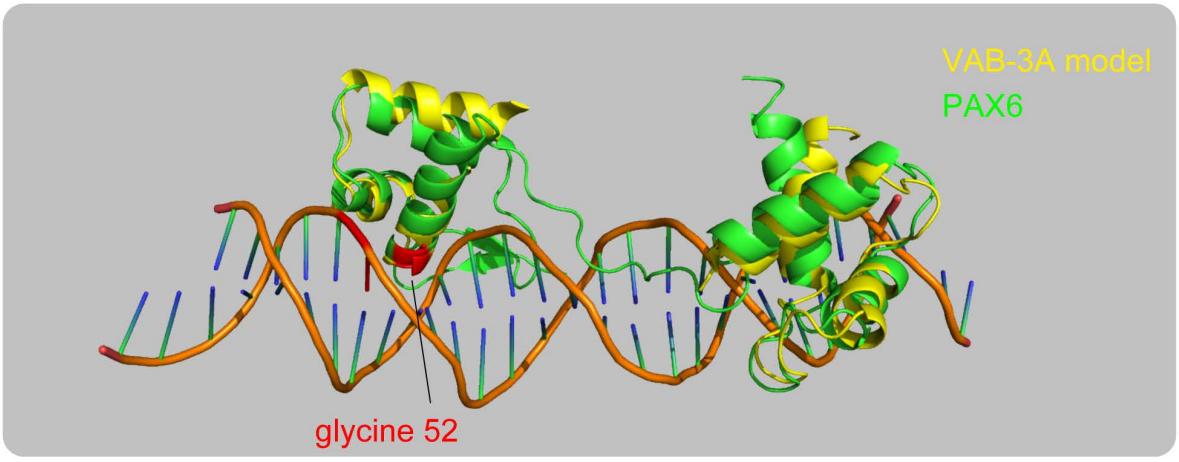

Figure S2. *wz25* affects a highly conserved residue in the VAB-3A Paired homology domain.
A. Radial dendrogram showing relatedness of VAB-3A to Paired domain-containing proteins from mouse (*Mus musculus)* and fly (*Drosophila melanogaster*).
B**.** ClustalW alignment of Paired domain sequences showing the conservation of the glycine (G52) predicted to be affected by the *wz25* mutation.
C. Homology model of the VAB-3A Paired domain based on the crystal structure of mouse Pax6 bound to DNA determined by Xu *et al.* (1999). The residue mutated by *wz25* is likely part of a helix that mediates interactions with DNA. A homology model of VAB-3A structure was generated using the Phyre2 server (Kelley et al., 2015) and visualized using MacPyMol (Schrodinger LLC).

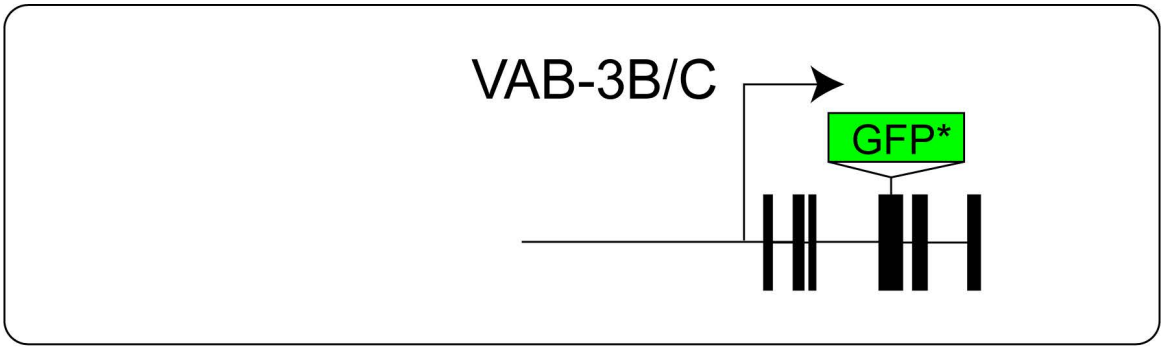

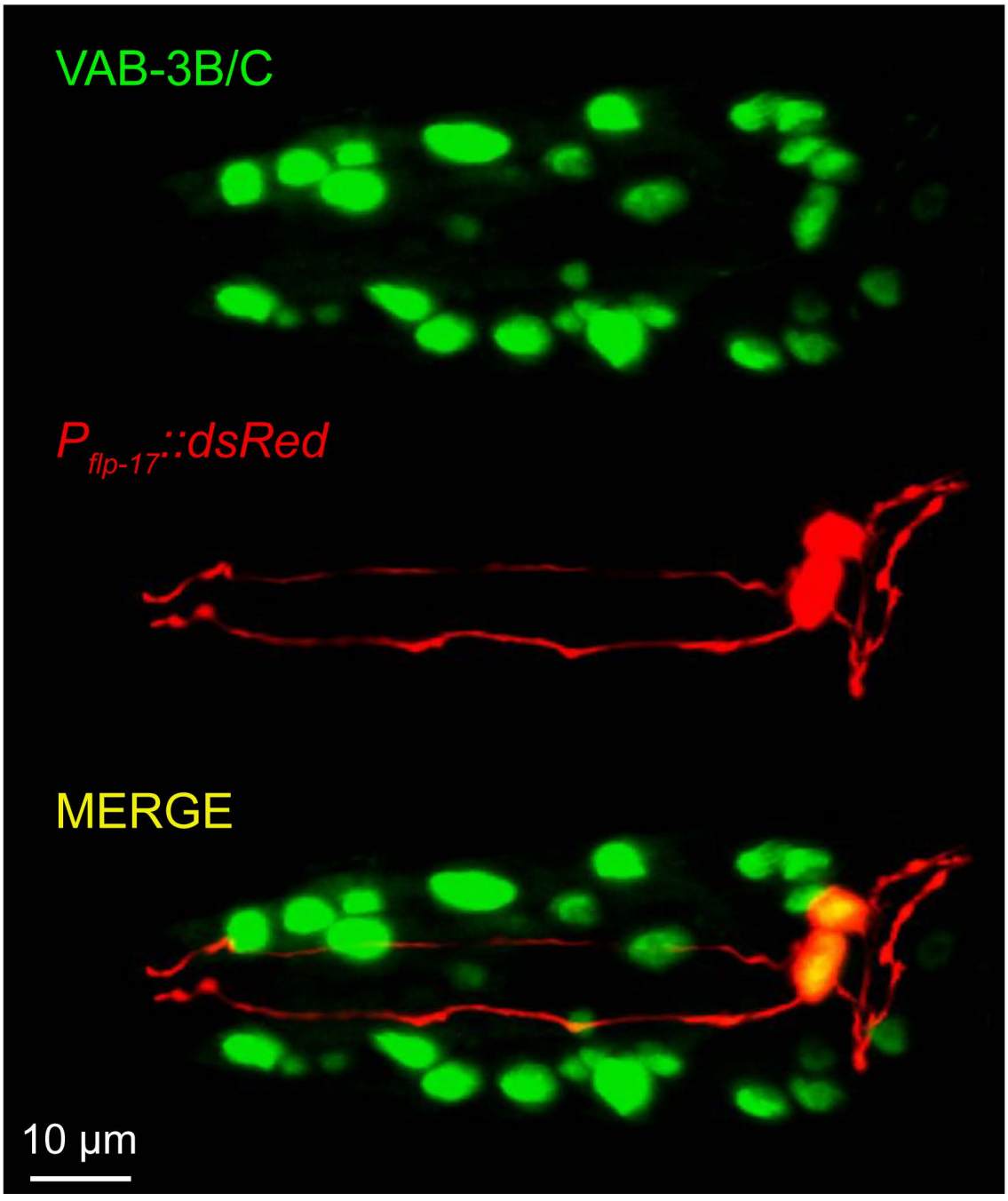

Figure S3. The VAB-3 short isoforms are expressed in head cells including BAG.
Schematic of reporter for expression of short (VAB-3B/C) isoforms of *vab-3*. An adult hermaphrodite expressing a VAB-3B/C transcriptional reporter and $P_{flp\text{-}17}$*::dsRed*.

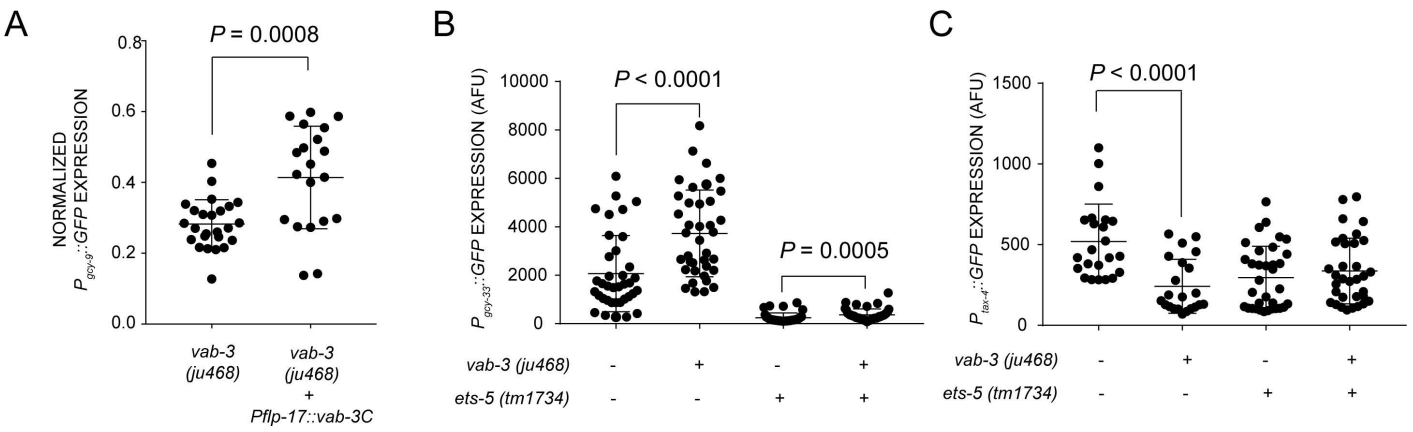

Figure S4. A mutation affecting the short isoforms of VAB-3 has different effects on BAG-enriched genes.

A. Levels of P_{gcy-9}*::GFP*-expression in BAG neurons of *vab-3* mutants in Arbitrary Fluorescence Units (AFU) normalized to the wild type average. BAG-specific expression of the short isoform in *ju468* partially rescues *gcy-9* expression.

B. Levels of P_{gcy-33}*::GFP*-expression in BAG neurons of *vab-3* mutants in Arbitrary Fluorescence Units (AFU). *ju468*, an allele affecting the short isoform, causes increased levels of the BAG-specific guanylate cyclase, and it also suppresses the decrease in P_{gcy-33}*::GFP* caused by *ets-5*.

C. Levels of P_{tax-4}*::GFP*-expression in BAG neurons of *vab-3* mutants. *ju468* causes decreased levels of the cyclic nucleotide-gated calcium channel subunit, yet no additive decrease in an *ets-5* mutant background.

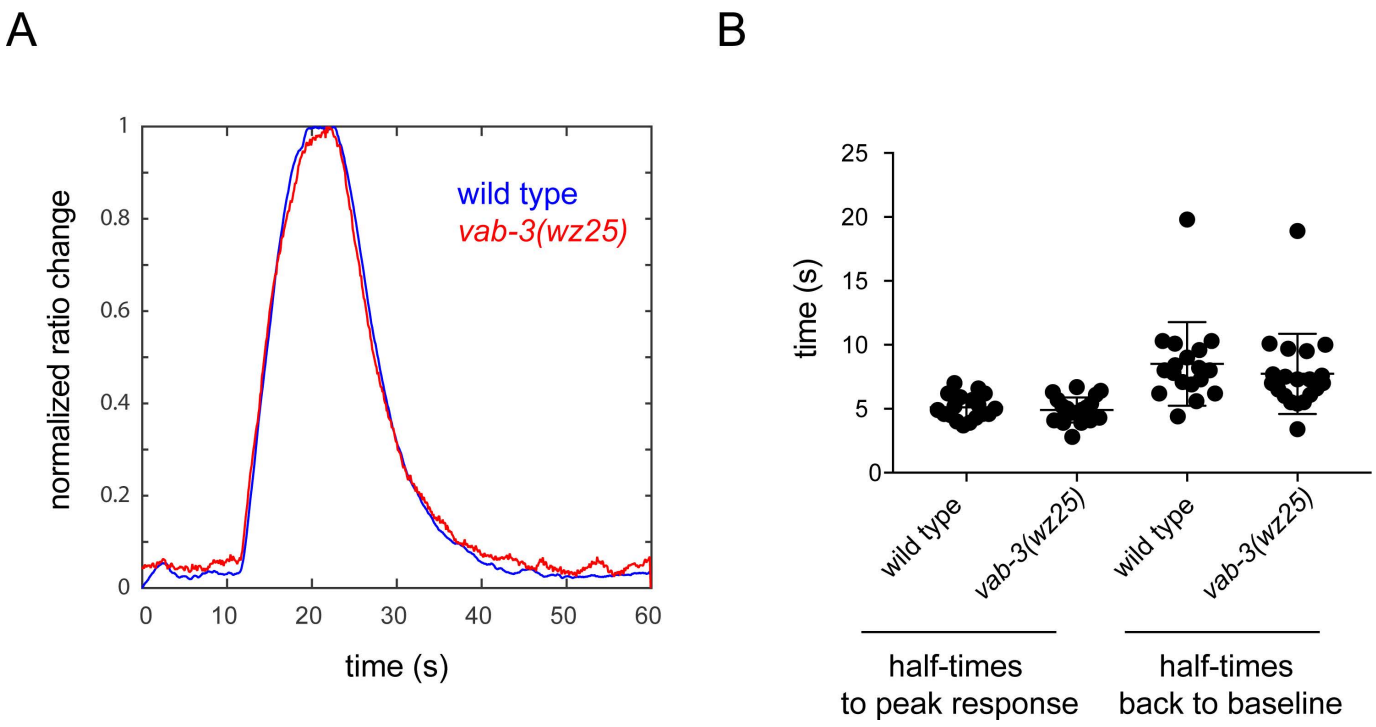

Figure S5. Dynamics of BAG neuron calcium transients.
A. The average calcium responses of wild-type and *wz25* BAG neurons scaled to unity. A 10 s pulse of 10% CO_2 was delivered at the 10-second mark.
B. Rise-times (half-times to peak after stimulus onset) and recovery times (half-times to baseline after stimulus is removed) of wild-type and *wz25* mutant BAG neurons stimulated with 10% CO_2. Bars in scatterplots display mean ± SD.

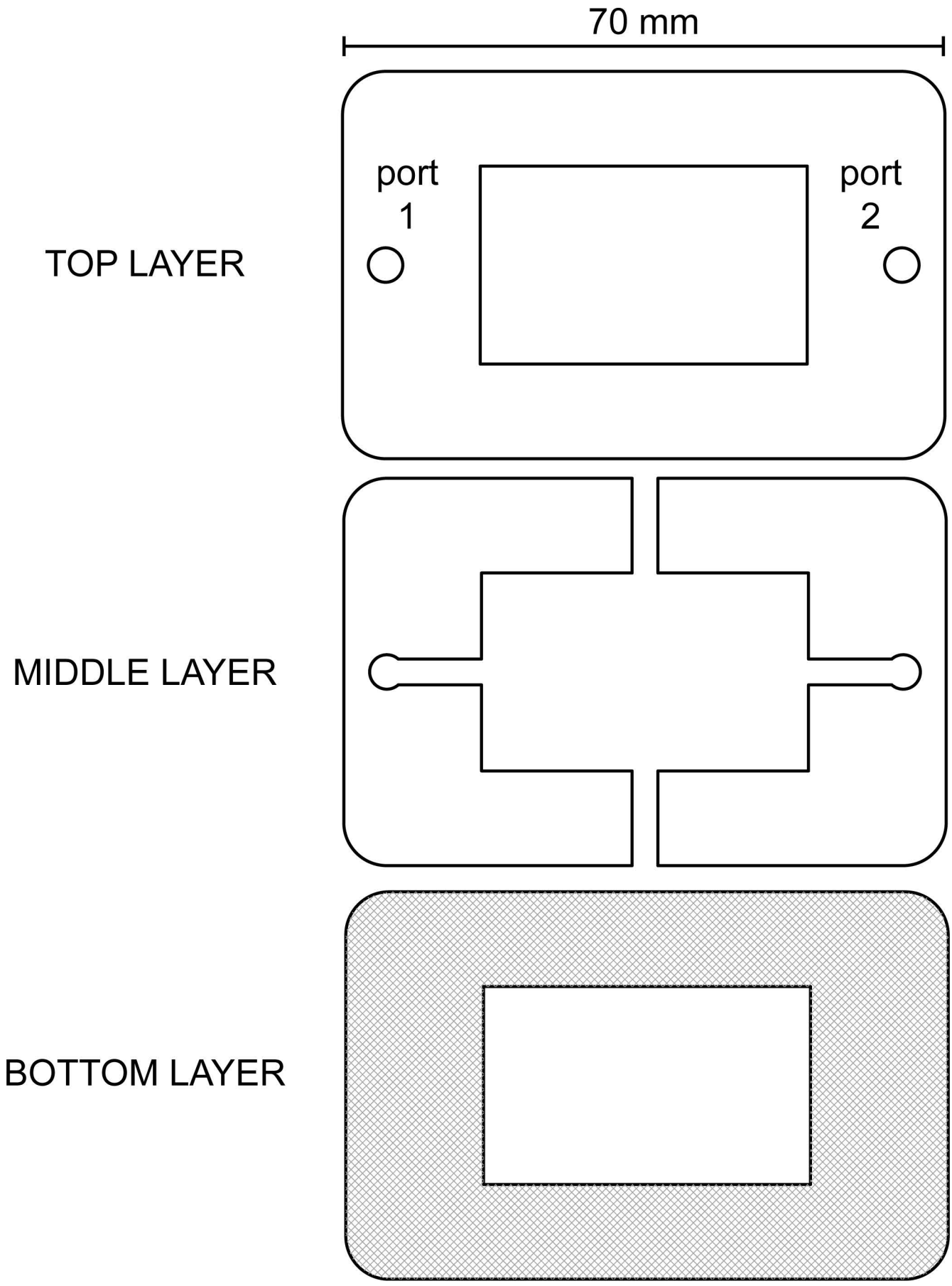

Figure S6. Design and construction of chemotaxis chambers used in this study
Chemotaxis chambers were constructed by adhering three layers that were laser-cut from 1/16" acrylic sheet plastic. The bottom layer was etched with a hatched pattern, shown in gray. This hatching generated a textured surface on the bottom of the chamber. After the top and middle layers were bonded, ports were tapped to received plastic barbed fittings to which plastic tubing was attached. The fully assembled chamber was covered with a rectangular coverglass adhered to the chamber with silicone grease. The textured bottom of the chamber was painted with glycerol to adhere it to the surface of NGM agar plates and to generate a barrier that confined worms within the chamber. Original CAD files are available upon request.

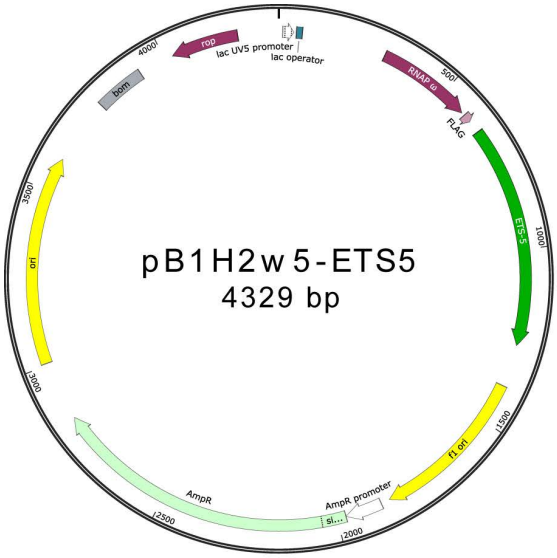

>ETS-5 B1H BAIT
MQYASALSRIPSSNSTSASKGPMAIALSATGTGQIQ
LWQFLLELLADAVNAHCIAWEGSNGEFKLVDPDEV
ARKWGERKSKPNMNYDKLSRALRYYYDKNIMTKV
QGKRYAYKFDFQGLAQACQSAILTNGGNPNGDLSS
TVHSLSPYTNQVLPIGVTSRLSTSMSSYHSILSSTS
STSSNQIIPPSTATYWSTPQSSLTYTGMPSSY*

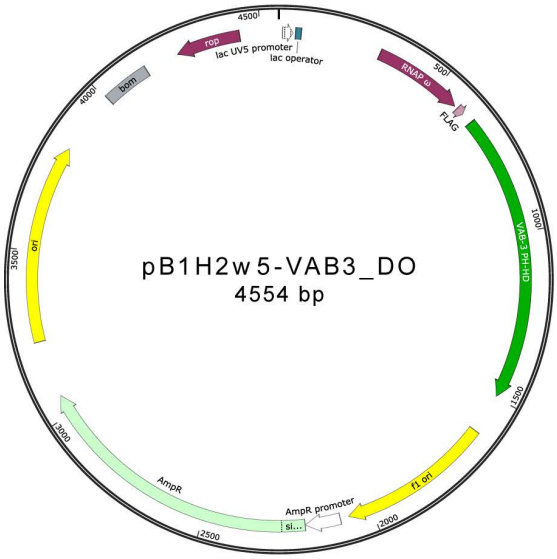

>VAB-3 B1H BAIT
TSDAGHTGVNQLGGVFVNGRPLPDATRQRIVDLA
HKGCRPCDISRLLQVSNGCVSKILCRYYESGTIRPR
AIGGSKPRVATSDVVEKIEDYKRDQPSIFAWEIRDK
LLADNICNNETIPSVSSINRVLRNLAAKKEQVTMQT
ELYDRIRIVDNFPYNSSWYGQWPIPMNGAVGLNPF
VPAPLIEPKTEGEFEKDEDQKPPTEPEDDAAARMR
LKRKLQRNRTSFTQVQIESLEKEFERTHYPDVFAR
ERLAQKIQLPEARIQVWFSNRRAKWRREEKMRNK
RSS*

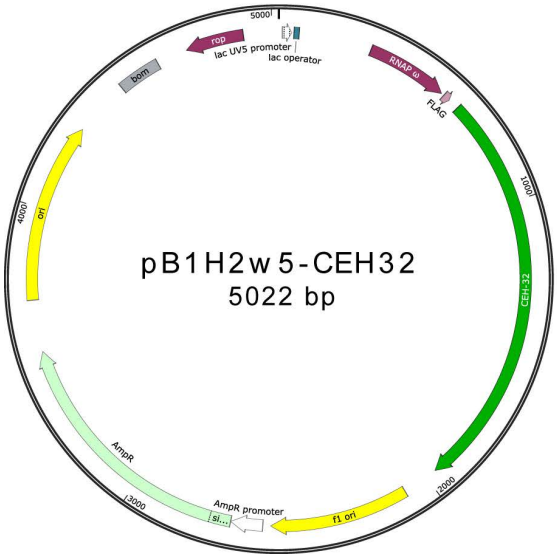

>CEH-32 B1H BAIT
MFTPEQFTKVMSQLGNFSQLGQMFQPGNVAMLQ
ALQANGASSTPSLFPAMPSVIPSLAAPSSPTTSNLT
ADQIVKTCEQLETDGDVDGLFRFMCTIPPQKTQEV
AGNEAFLRARALVCFHASHFRELYAILENNKFSPKY
HPKLQEMWHEAHYREQEKNRGKSLCAVDKYRVR
KKYPMPRTIWDGEQKTHCFKERTRSLLREWYLKD
PYPNPPKKKELANATGLTQMQVGNWFKNRRQRD
RAAAAKNKQNIIGVELKKTSSDMSDSDDDFEDSMT
DSPSPIDEPKDLSKSHIPKLSPTLLPKMATPFDMFA
AAANPLMMLNLNPALYMQFHNFFNTMRNPQIDEEE
NSETTVEVEADIEPPKKRSKLSIDEILNIKSEVSPSQ
CSPCSNESLSPKRAVKTEEVKKEDDEAAEEDSRSV
KSETSEDPKHSSPKSTTSQSE*

Figure S7. Sequences of baits used for bacterial one-hybrid screens
Schematics of plasmids used to express ETS-5, VAB-3, and CEH-32 for bacterial one-hybrid screening. The amino acid sequences of the baits encoded by each plasmid are shown to the right.